



Universiteit
Leiden
The Netherlands

Quantification of endocannabinoids in human cerebrospinal fluid using a novel micro-flow liquid chromatography-mass spectrometry method

He, B.S.; , X.Y. di; Guled, F.; Harder, A.V.E.; Maagdenberg, A.M.J.M. van den; Terwindt, G.M.; ... ; Hankemeier, T.

Citation

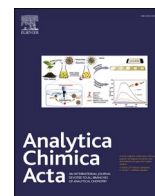
He, B. S., Guled, F., Harder, A. V. E., Maagdenberg, A. M. J. M. van den, Terwindt, G. M., Krekels, E. H. J., ... Hankemeier, T. (2022). Quantification of endocannabinoids in human cerebrospinal fluid using a novel micro-flow liquid chromatography-mass spectrometry method. *Analytica Chimica Acta*, 1210, 339888. doi:10.1016/j.aca.2022.339888

Version: Publisher's Version

License: [Creative Commons CC BY 4.0 license](#)

Downloaded from: <https://hdl.handle.net/1887/3513929>

Note: To cite this publication please use the final published version (if applicable).



Quantification of endocannabinoids in human cerebrospinal fluid using a novel micro-flow liquid chromatography-mass spectrometry method

Bingshu He^{a,1}, Xinyu Di^{a,1}, Faisa Guled^a, Aster V.E. Harder^{b,c},
 Arn M.J.M. van den Maagdenberg^{b,c}, Gisela M. Terwindt^b, Elke H.J. Krekels^a,
 Isabelle Kohler^{d,e}, Amy Harms^a, Rawi Ramautar^{a,*}, Thomas Hankemeier^{a,**}

^a Division of Systems Biomedicine and Pharmacology, Leiden Academic Centre for Drug Research, Leiden University, Leiden, the Netherlands

^b Department of Neurology, Leiden University Medical Center, Leiden, the Netherlands

^c Department of Human Genetics, Leiden University Medical Center, Leiden, the Netherlands

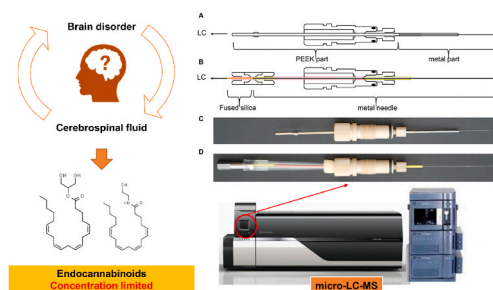
^d Division of BioAnalytical Chemistry, Vrije Universiteit Amsterdam, Amsterdam Institute of Molecular and Life Sciences (AIMMS), Amsterdam, the Netherlands

^e Center for Analytical Sciences Amsterdam, Amsterdam, the Netherlands

HIGHLIGHTS

- Modification on spray needle made to improve robustness of micro-LC-MS system.
- Limit of detection of anandamide as low as 0.7 pM, while limit of quantification could reach 2.4 pM.
- Method applied to the determination of endocannabinoids in 288 human CSF samples.

GRAPHICAL ABSTRACT



ARTICLE INFO

Keywords:

Endocannabinoids
 Cerebrospinal fluid
 Micro-LC-MS
 Down-scaling analysis

ABSTRACT

The endocannabinoid system (ECS) is implicated in various brain disorders. Changes in the composition of the cerebrospinal fluid (CSF) may be associated with ECS-related pathologies. Endocannabinoids (eCBs) and their analogues are present at low concentrations in human CSF, which hampered the investigation of the ECS in this body fluid. In this study, we developed a highly sensitive and selective micro-flow liquid chromatography-tandem mass spectrometry (micro-LC-MS/MS) method for the analysis of eCBs and eCB analogues in human CSF. The developed method allowed for the quantitative analysis of 16 eCBs and their analogues in human CSF. Micro-LC-MS/MS analyses were performed at a flow-rate of $4 \mu\text{L min}^{-1}$ with a 0.3-mm inner diameter column. A minor modification of a novel spray needle was carried out to improve the robustness of our method. By using an injection volume of $3 \mu\text{L}$, our method reached limits of detection in the range from 0.6 to 1293.4 pM and limits of quantification in range from 2.0 to 4311.3 pM while intra- and interday precisions were below 13.7%. The

* Corresponding author. Biomedical Microscale Analytics, Leiden Academic Centre for Drug Research (LACDR), Leiden University, Einsteinweg 55, 2333 CC, Leiden, the Netherlands.

** Corresponding author. Division of Systems Biomedicine and Pharmacology, Leiden Academic Centre for Drug Research (LACDR), Leiden University, Einsteinweg 55, 2333 CC, Leiden, the Netherlands.

E-mail addresses: r.ramautar@lacdr.leidenuniv.nl (R. Ramautar), hankemeier@lacdr.leidenuniv.nl (T. Hankemeier).

¹ These authors contributed equally to this work.

<https://doi.org/10.1016/j.aca.2022.339888>

Received 4 February 2022; Received in revised form 13 April 2022; Accepted 28 April 2022

Available online 2 May 2022

0003-2670/© 2022 The Authors. Published by Elsevier B.V. This is an open access article under the CC BY license (<http://creativecommons.org/licenses/by/4.0/>).

developed workflow was successfully used for the determination of eCBs in 288 human CSF samples. It is anticipated that the proposed approach will contribute to a deeper understanding of the role of ECS in various brain disorders.

1. Introduction

The endocannabinoid system (ECS) is a widely distributed signaling system in the brain, involving cannabinoid receptors 1 and 2 (CB1 and CB2) and their best known endogenous agonists *N*-arachidonoyl ethanolamine (anandamide, AEA) and 2-arachidonoyl glycerol (2-AG), which are defined as endocannabinoids (eCBs) [1]. Besides AEA and 2-AG, other structural analogues, i.e., other *N*-acyl ethanolamines (NAEs) and other 2-acylglycerols play important roles in ECS signaling, by enhancing the effects of AEA and 2-AG via increasing receptor affinity or inhibiting hydrolysis, known as the ‘entourage effect’ [2,3].

Alterations in the ECS have been reported in experimental models of various brain disorders, including Alzheimer’s disease, Parkinson’s disease, and migraine [4–7]. To certain extent, the reported findings were supported by those obtained in clinical studies [8–10]. However, most of the clinical studies used plasma or postmortem tissue samples, which limits the validity of ECS findings. Due to its close connection with brain tissue, cerebrospinal fluid (CSF) represents a more suitable biospecimen. Indeed, CSF reflects the level of metabolites in brain and is thus believed to better capture the brain’s neurochemistry compared to blood. However, eCBs and their analogues in human CSF, especially AEA, are present at concentrations lower than picomolar or even femtomolar range [11–17], highlighting the need for adequate methods to reliably detect and quantify these compounds [18–20]. In studies reporting endogenous concentrations of eCBs and eCB analogues in human CSF [14–17,20,21], relatively large volumes of CSF (≥ 1 mL) were needed to reach the required sensitivity.

Using low-flow rate ranges between 1 and 50 $\mu\text{L min}^{-1}$, micro-flow LC leads to the formation of smaller and more uniform spray droplets during the electrospray ionization process, improving the ionization efficiency significantly. Moreover, with the smaller inner diameter columns that are typically used (75 μm –1 mm-I.D.), micro-flow LC-MS provides higher sensitivity using lower amounts of sample. Since human CSF samples are difficult to obtain, a more sensitive method to make optimal use of such samples is required. Kantae et al. [19] developed a quantitative method based on a chip-based nano-LC-MS system for the analysis of eCBs in CSF. Using only 200 μL of human CSF, the method provided a limit of detection (LOD) from 0.3 to 61.2 pM. Intra- and inter-assay variability (expressed by the coefficient of variation, CV) varied from 2 to 23% and 3–21%, respectively. However, due to the small inner diameter of the spray emitter, the LC tubing, and the column, the overall stability of such chips remains a challenging aspect in nano-flow LC-MS, contrary to conventional methods with 2.1-mm columns and milliliter range flow rates [22,23]. In addition, the chips used in the study of Kantae et al. are no longer commercially available, showing the need for an alternative method.

In this study, we developed a sensitive and robust micro-LC-MS/MS method for the simultaneous absolute quantification of eCBs and their analogues in human CSF. To improve robustness, the spray needle in the commercial micro spray ion source was modified to avoid clogging. The overall sensitivity was compared between conventional and micro-flow

rates. Parameters were optimized for several flow rates and a final method using 4 $\mu\text{L min}^{-1}$ as flow rate and a 0.3-mm inner diameter column was selected. The method was validated based on the guidance of bioanalytical method validation from EMA(2009) [24] for the quantification of eCBs. The validated method was applied to 288 human CSF samples with acceptable performance metrics, thereby demonstrating the value of this method for future studies focusing on deciphering the involvement of ECS in brain disease.

2. Material and methods

2.1. Chemicals and materials

LC-MS-grade acetonitrile (ACN) and formic acid were purchased from Biosolve B.V. (Valkenswaard, Netherlands). Anhydrous methyl *tert*-butyl ether (MTBE, $\geq 99.8\%$), ammonium acetate ($\geq 99.0\%$) and ammonium formate ($\geq 99.9\%$) were purchased from Sigma-Aldrich (St. Louis, Missouri, United States). Purified water was obtained from a Milli-Q PF Plus system (Merck Millipore, Burlington, Massachusetts, United States).

The standard reagents α -linolenoyl ethanolamide (α -LEA), palmitoleoyl ethanolamide (POEA), pentadecanoyl ethanolamide (PDEA), linoleoyl ethanolamide (LEA), anandamide (AEA), docosahexaenoyl ethanolamide (DHEA), 1-arachidonoylglycerol (1-AG), 2-arachidonoylglycerol (2-AG), 1-linoleoyl glycerol (1-LG), 2-linoleoyl glycerol (2-LG), palmitoyl ethanolamide (PEA), dihomogamma-linolenoyl ethanolamide (DGLEA), docosatetraenoyl ethanolamide (DEA), 1-oleoyl glycerol (1-OG), 2-oleoyl glycerol (2-OG), stearoyl ethanolamide (SEA), eicosapentaenoyl ethanolamide (EPEA), mead acid ethanolamide (ETAEA), *N*-oleoylethanolamine (OEA) and deuterated standards *N*-(2-hydroxyethyl-1,1,2,2-d₄)-9Z,12Z-octadecadienamide (LEA-d₄), *N*-(2-hydroxyethyl-1,1',2,2'-d₄)-4Z,7Z,10Z,13Z,16Z,19Z-docosahexaenamide (DHEA-d₄), *N*-(2-hydroxyethyl)-5Z,8Z,11Z,14Z-eicosatetraenamide-5,6,8,9,11,12,14,15-d₈ (AEA-d₈), 5Z,8Z,11Z,14Z-eicosatetraenoic-5,6,8,9,11,12,14,15-d₈ acid (2-AG-d₈), *N*-(2-hydroxyethyl)-hexadecanamide-7,7,8,8-d₄ (PEA-d₄), *N*-(2-hydroxyethyl)-octadecanamide-18,18,18-d₃ (SEA-d₃) and *N*-(2-hydroxyethyl-1',1,2,2'-d₄)-9Z-octadecanamide (OEA-d₄) were purchased from Cayman Chemical (Ann Arbor, Michigan, United States).

2.2. Preparation of standards and internal standards solutions

Pure standards ($>98\%$ purity) at different stock concentrations were dissolved in ethanol or ACN. The standard stock solutions were diluted to 1 mM using ACN. Standard solution I, used for direct infusion experiments, included 5 nM of each compound in group A (AEA, DEA, DGLEA, DHEA, ETAEA, LEA, EPEA, PDEA, POEA and α -LEA), 50 nM of each compound in group B (2-AG, 1-AG, SEA, OEA, and PEA) and 500 nM of each compound in group C (2-LG, 1-LG, 2-OG, 1-OG). Standard solution II was obtained by diluting standard solution I four times with ACN and used for LC-MS method development.

Table 1
Concentrations of eCBs and eCB analogues standards in calibrant solutions.

Compound group	Concentration (pM)									
	C0	C1	C2	C3	C4	C5	C6	C7	C8	C9
A	0	7.3	14.65	29.3	58.6	117.2	468.8	1875	3750	7500
B	0	73.3	146.5	293.0	586.0	1171.9	4687.5	18750	37500	75000
C	0	732.4	1464.9	2929.7	5859.4	11718.8	46875	187500	375000	750000

Table 2

Experimental conditions used for performance comparison of different flow rates.

	Conventional flow		Micro-flow	
	Flow rate	550 $\mu\text{L min}^{-1}$	250 $\mu\text{L min}^{-1}$	100 $\mu\text{L min}^{-1}$, 50 $\mu\text{L min}^{-1}$
Syringe (for direct infusion)	Hamilton Gastight #1001		Hamilton Gastight #1750	
Syringe pump LC	Harvard Apparatus Model 22		Waters nanoAcquity	
Column	Shimadzu Nexera X2 LC-30AD		Phenomenex C18 (2.6 μm , 0.3 \times 50 mm)	
Ionization source (For both direct infusion and LC-MS analysis)	Waters BEH C18 (1.7 μm , 2.1 \times 50 mm)	SCIEX Turbo V with a 100- μm I.D. emitter	SCIEX Turbo V with a 100- μm I.D. emitter	SCIEX Turbo V with a 50- μm I.D. emitter

The deuterated internal standard (ISTD) working solution containing 225.3 nM 2-AG- d_8 , 4.5 nM AEA- d_8 , 0.6 nM DHEA- d_4 , 3.0 nM LEA- d_4 , 6.0 nM OEA- d_4 , 0.6 nM PEA- d_4 and 12 nM SEA- d_3 was prepared in ACN. All the standard solutions were stored at -20°C .

2.3. Preparation of calibrant solutions

Each standard stock solution (1 mM) was mixed and diluted in ACN, resulting in nine calibration concentration levels. For each calibration level, 10 μL of each solution was mixed with ISTD working solution to reach the adequate concentration. The concentrations of ISTDs were chosen to be in the middle of the dynamic range, i.e., equivalent to C4 concentration. Final concentrations of all compounds are shown in Table 1.

2.4. Collection of human CSF samples

CSF samples were collected via a lumbar puncture (LP) in a randomized fashion between 2008 and 2016 and between 9:00 a.m. and 1:00 p.m. to minimize diurnal and seasonal variation. The protocol was approved by the ethics committee of Leiden University Medical Center. The LP was performed between the L3/L4, L4/L5 or L5/S1 interspace, whereby 3 mL CSF was sampled directly in a 15-mL polypropylene Falcon tube (Cat. No. 188271; Greiner) that already contained 6 mL of cold ethanol and was placed in an ice bath. Ethanol was used to stabilize the metabolites during long-term storage. After the collection of CSF, the tube was gently shaken and immediately put back on ice. Subsequently, the CSF was divided in aliquots of 1.5 mL in 1.8-mL cryotubes (Art. No. 368632; NUNC Brand). The cryotubes were placed on dry ice within 40 min of sampling and immediately transferred to -80°C . All CSF samples remained at -80°C until analysis.

2.5. Sample preparation

The sample preparation was carried out using 750 μL of the mixture of CSF and ethanol (including 500 μL ethanol). Samples were evaporated using a SpeedVac (Thermo Fisher, USA) for 90 min to remove ethanol. Next, 1 mL of MTBE, 50 μL 0.1 M ammonium acetate solution at pH 4 buffer solution and 10 μL ISTD working solution were added to each sample, followed by 10 min of standard vortex and centrifugation. After 5 min, the organic layer was transferred to a 1.5-mL Eppendorf tube and evaporated to dryness. Samples were reconstituted in 20 μL of a mixture of water/ACN (1:1, v/v), vortexed for 20 min and centrifuged at 16,000 g for 10 min. Finally, 15 μL of supernatant was transferred in an

Table 3

Validation parameters: calibration range, retention time, LODs, and LOQs.

Compound	Calibration ranges (pM)	Retention time (min)	R ²	LOD (pM)	LOQ (pM)
α -LEA	29.3–7500	10.0	0.9978	3.5	11.8
EPEA	58.6–7500	10.0	0.9980	15.1	50.4
POEA	14.6–7500	10.4	0.9970	2.6	8.7
PDEA	7.3–7500	10.8	0.9978	2.1	7.0
DHEA	58.6–7500	10.8	0.9963	34.4	114.6
AEA	7.3–7500	10.9	0.9982	0.7	2.4
LEA	29.3–7500	11.0	0.9983	14.8	49.3
DGLEA	29.3–7500	11.5	0.9975	2.0	6.5
1-AG/2-AG	146.5–75000	11.6/11.8	0.9965	0.6	2.0
1-LG/2-LG	1464.8–750000	11.7/11.9	0.9957	3.2	10.5
PEA	585.9–75000	11.7	0.9933	1293.4	4311.3
ETAEA	29.3–7500	11.9	0.9966	14.1	46.9
OEA	73.2–75000	12.0	0.9988	5.3	17.8
DEA	7.3–7500	12.1	0.9965	1.3	4.4
1-OG/2-OG	5859.4–750000	12.5/12.7	0.9976	45.7	152.4
SEA	146.5–75000	13.0	0.9963	29.5	98.3

*R², coefficient of determination.

autosampler vial and injected into the LC-MS instrument.

2.6. Optimization of micro-flow rates and comparison with UHPLC-MS

During the performance comparison evaluation of different flow rates, direct infusion to mass spectrometer and LC-MS methods were used. Direct infusion MS was performed using a syringe pump connected to SCIEX QTRAP 6500+ mass spectrometer (SCIEX, Framingham, Massachusetts, United States). A Shimadzu Nexera X2 LC-30AD system (Shimadzu corporation., Kyoto, Japan) and Waters nanoAcquity LC system (Waters, Milford, Massachusetts, United States) were used for high- and micro-flow rates, respectively. Various columns and ionization sources suited for each flow rate were chosen to allow for an adequate comparison (Table 2). Moreover, UHPLC-MS/MS and micro-LC-MS/MS parameters in this comparison experiment were also optimized for each flow rate and can be found in Supplemental Table S1.

2.7. Micro-LC-MS/MS instrumentation and conditions

The micro-LC-MS/MS analyses were performed using a Waters nanoAcquity LC instrument coupled to a Shimadzu LCMS-8060 triple quadrupole mass spectrometer equipped with a micro-ionization source (Shimadzu corporation., Kyoto, Japan) and an optimized spray needle, i.e., 15-cm Metal TaperTip™ emitter with 30- μm tip inner diameter (New Objective, Littleton, Massachusetts, United States). The separation was carried out using a Phenomenex C18 column (2.6 μm , 0.3 \times 150 mm) maintained at 45°C . The injection volume was 3 μL . Eluent A was composed of 2 mM ammonium formate with 10 mM formic acid in water, and eluent B was ACN. Using a flow rate of 4 $\mu\text{L min}^{-1}$, the initial gradient started at 55% eluent B and maintained for 0.5 min, eluent B was increased to 60% from 0.5 to 1.5 min, increased to 70% from 1.5 to 2.0 min, to 85% from 2.0 to 5.5 min, and increased to 95% at 5.6 min, where the gradient was kept until 8.0 min, then decreased to 55% eluent B at 8.1 min. The column was equilibrated for 8 min until the next injection, giving a total analysis time of 16 min. MS data was acquired in positive ionization mode with nebulizing gas flow rate of 0.2 L min^{-1} , interface voltage at 2 kV, interface temperature at 58°C , and desolvation line (DL) temperature at 250°C . Selected reaction monitoring (SRM) was used for data acquisition by monitoring the precursor-product ion transitions as indicated in Supplemental Table S2. These instruments and conditions were used during method validation and application on CSF samples.

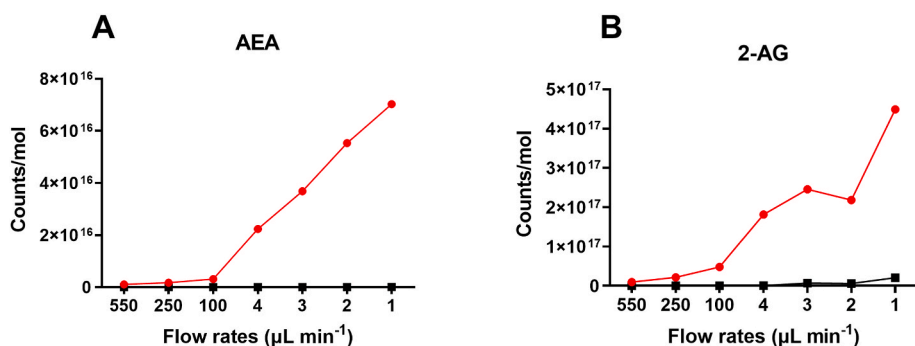


Fig. 1. Effect of different flow rates on sensitivity of (A) AEA and (B) 2-AG with direct infusion to SCIEX Qtrap 6500+ with Sciex Turbo V ionization source ($100\text{--}550\ \mu\text{L min}^{-1}$) and NanosprayIII ionization source ($1\text{--}4\ \mu\text{L min}^{-1}$). Red line: infusion of standard solution I with 5 nM AEA and 50 nM 1-AG/2-AG in 70% ACN. Black line: infusion of blank sample containing 70% ACN. The y-axis shows the signal as counts per mol, x-axis shows flow rates. MS parameters are listed in [Supplemental Table S1](#). (For interpretation of the references to color in this figure legend, the reader is referred to the Web version of this article.)

2.8. Method validation

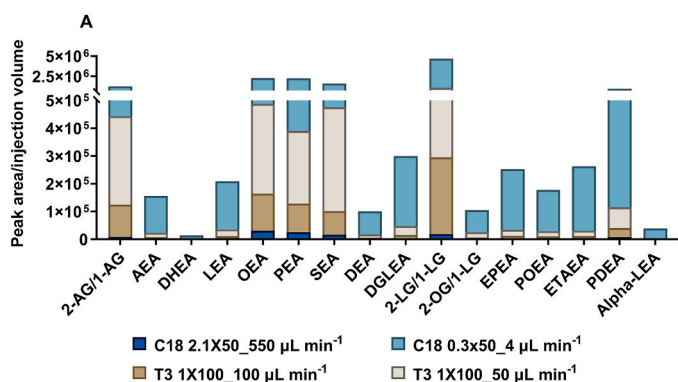
Linearity and limit of detection Linearity was evaluated by preparing calibration lines ($n = 3$) on three consecutive days. The calibration ranges are shown in [Table 3](#). All calibration lines were fitted to a $1/x^2$ weighted linear regression model. The limits of detection (LOD) and limits of quantification (LOQ) were calculated as $\text{LOD} = 3 \times S_a/b$, $\text{LOQ} = 10 \times S_a/b$, where S_a is the standard deviation of the y-intercept, b is the slope of the calibration curve [25].

Precision The intra- and interday precisions were evaluated by spiking three different concentrations of ISTD solutions [low-level(C2), medium-level(C4) and high-level(C6)] into pooled CSF samples over three different days ($n = 3$). Precision was expressed as the RSD of the peak areas of ISTD. An RSD less than 15% was within the tolerance limits of the EMA guidelines [24].

Recovery and matrix effects Recovery and matrix effect were evaluated by spiking ISTD solutions to pooled CSF samples ($n = 3$) or water ($n = 3$). Recovery was calculated as the ratio of ISTD peak areas measured before and after extraction. Matrix effect was the ratio of spiked ISTD peak areas acquired within pooled CSF and water, both spiked after extraction.

2.9. Data preprocessing

LabSolutions LCMS Version 5.97 SP1 (Shimadzu, Japan) and SCIEX OS version 1.6 (SCIEX, United States) were used for peak picking and integration. Absolute quantitation was calculated using the equation of the calibration curve and using the peak area ratios (peak area of targeted analyte divided by peak area of respective ISTD). F-test for linear regression was performed using Excel 2016.



3. Results and discussion

3.1. Optimization of micro-flow rates and comparison with UHPLC-MS

The main advantage of micro-LC is the ability to obtain similar or lower LODs compared with UHPLC, but with significantly reduced injection volumes, making this approach well-suited for analyzing compounds in biomass-restricted samples [26]. Another advantage of micro-LC is a higher robustness compared to nano-LC columns, which is key for clinical studies. In addition to the expected advantages of downscaling LC column diameters, such as higher sensitivity [27], micro-LC results in an improved ESI efficiency. Various flow rates were evaluated using direct infusion MS and micro-LC-MS analysis of eCBs to evaluate the improvement in ESI efficiency. With direct infusion, various flow rates at conventional (i.e., $550\ \mu\text{L min}^{-1}$, $250\ \mu\text{L min}^{-1}$, $100\ \mu\text{L min}^{-1}$) and micro-level (i.e., $4\ \mu\text{L min}^{-1}$, $3\ \mu\text{L min}^{-1}$, $2\ \mu\text{L min}^{-1}$, $1\ \mu\text{L min}^{-1}$) range were investigated, with optimized parameters on the same MS instrument. After allowing the flow rates to stabilize, a time window of 1 min was picked and data within this window was summed. The sensitivity of each flow rate was expressed as counts per mole. As shown in [Fig. 1](#), significant improvements of the sensitivity were observed for both AEA and 2-AG as the flow rate decreased, especially at the low $\mu\text{L min}^{-1}$ flow rates. This observation is in line with previously reported findings, in which the sensitivity improvement at lower flow rates was attributed to an improved ionization efficiency [28]. It is worth mentioning that, although the increasing trends were still sharp when the flow rate changed to $1\ \mu\text{L min}^{-1}$, a noticeable increase of background noise was also observed, which may affect the signal-to-noise ratio in the LC-MS analysis.

Subsequently, the effect of flow rates was investigated using three micro-LC columns of different inner diameters. Based on the column capacity, four different flow rates from $550\ \mu\text{L min}^{-1}$ to $4\ \mu\text{L min}^{-1}$ were investigated using three columns with inner diameters of 2.1 mm, 1 mm and 0.3 mm, respectively ([Table 2](#)). The injection volumes of standard solution II on the three columns were 10 μL , 5 μL , and 0.5 μL ,

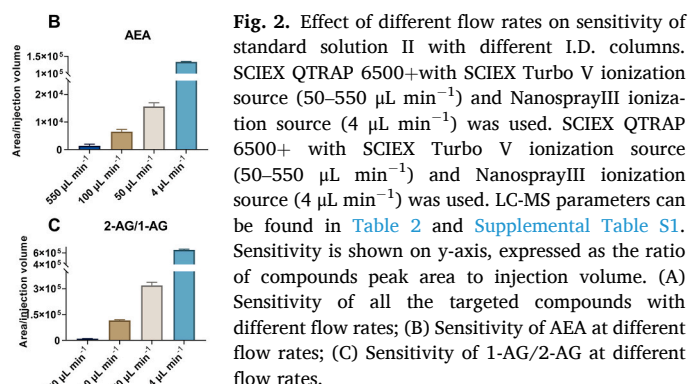


Fig. 2. Effect of different flow rates on sensitivity of standard solution II with different I.D. columns. SCIEX QTRAP 6500+ with SCIEX Turbo V ionization source ($50\text{--}550\ \mu\text{L min}^{-1}$) and NanosprayIII ionization source ($4\ \mu\text{L min}^{-1}$) was used. SCIEX QTRAP 6500+ with SCIEX Turbo V ionization source ($50\text{--}550\ \mu\text{L min}^{-1}$) and NanosprayIII ionization source ($4\ \mu\text{L min}^{-1}$) was used. LC-MS parameters can be found in [Table 2](#) and [Supplemental Table S1](#). Sensitivity is shown on y-axis, expressed as the ratio of compounds peak area to injection volume. (A) Sensitivity of all the targeted compounds with different flow rates; (B) Sensitivity of AEA at different flow rates; (C) Sensitivity of 1-AG/2-AG at different flow rates.

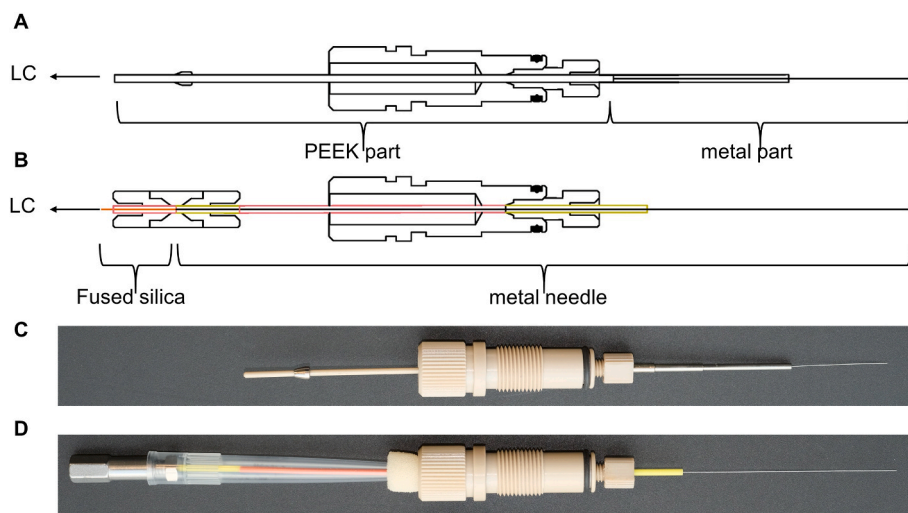


Fig. 3. Illustration of (A) the original spray needle and (B) the optimized spray needle; Pictures of (C) original spray needle and (D) optimized spray needle.

respectively. The dilution fold of injected sample under micro-flow rate was smaller, therefore, higher concentration of samples reached the MS interface. Fig. 2A shows that peak areas of all compounds significantly increased as the flow rates decreased. The detector response observed at each condition is expressed as the ratio of peak area to injection volume. As an example, at a flow rate of $4 \mu\text{L min}^{-1}$, the detector responses for AEA and 1-AG/2-AG were 9.7 and 9.4 times higher compared with responses observed at a flow rate of $550 \mu\text{L min}^{-1}$, respectively. The sensitivity for eCB analogues improved 5 to 22 times. The results confirm that the ionization efficiency of eCBs and eCB analogues can be enhanced by down-scaling flow rates using suitable columns.

In conclusion, a micro-flow LC-MS/MS method was able to increase the sensitivity of eCBs compared to a conventional UHPLC-MS/MS method. The MS signal is proportional to the amount of compounds reaching the detector within each unit of time, which demonstrates that micro-flow LC-MS analysis is concentration-dependent [29], where the lower the flow rate, the higher the signal. However, the robustness of the micro-flow method, when it reaches $1 \mu\text{L min}^{-1}$ or even the nano-flow level is crucial to consider. After taking the capacity of column, cycle time of the analysis, sensitivity required for quantification and most importantly, the method robustness into account, $4 \mu\text{L min}^{-1}$ was selected for the following experiments.

3.2. Micro-LC-MS/MS method development

Clogging in the tubing or spray needle remains a major obstacle during the development of low-flow rate LC-MS methods [30]. To avoid clogging and improve the ionization efficiency of the developed micro-LC-MS/MS method, we modified the micro-spray needles on the Shimadzu 8060. In the original micro-ion source, Shimadzu used a design called “UF-link™”. As shown in Fig. 3A and C, the original micro-spray needle consisted of a metal needle (opening I.D. = $50 \mu\text{m}$) and peak tubing, which were glued together. By connecting the peek tubing directly to the separation column, the dead volume from the connections and extra tubing was minimized. However, during practical use, the glued part was constantly clogged even when using standard solution injections under micro-flow rates. Since the ion source otherwise gave satisfactory performance, we decided to optimize the spray needle to fix the problem. After modification, the whole tubing part including peek part and metal part was removed and replaced by a 15-cm Metal TaperTip emitter ($30\text{-}\mu\text{m}$ tip opening and $360\text{-}\mu\text{m}$ outer diameter). This metal emitter was able to sustain robust performance for flow rates up to $5 \mu\text{L min}^{-1}$. At micro-flow rates, the influence of the volume in post-column tubing and unions on peak shape, especially peak

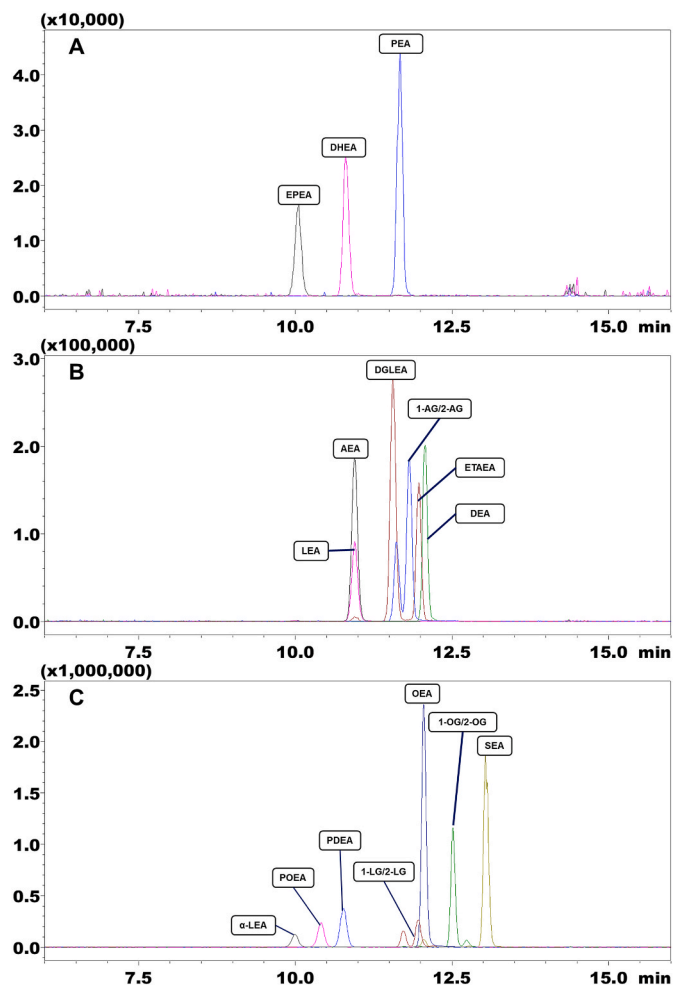


Fig. 4. Overlay of SRM chromatograms of eCBs and eCB analogues obtained with the injection of standard solution II. The three panels represent the same chromatogram in different scales. (A) Compounds with 1×10^4 scale intensity (B) compounds with 1×10^5 intensity scale (C) compounds with 1×10^6 intensity scale.

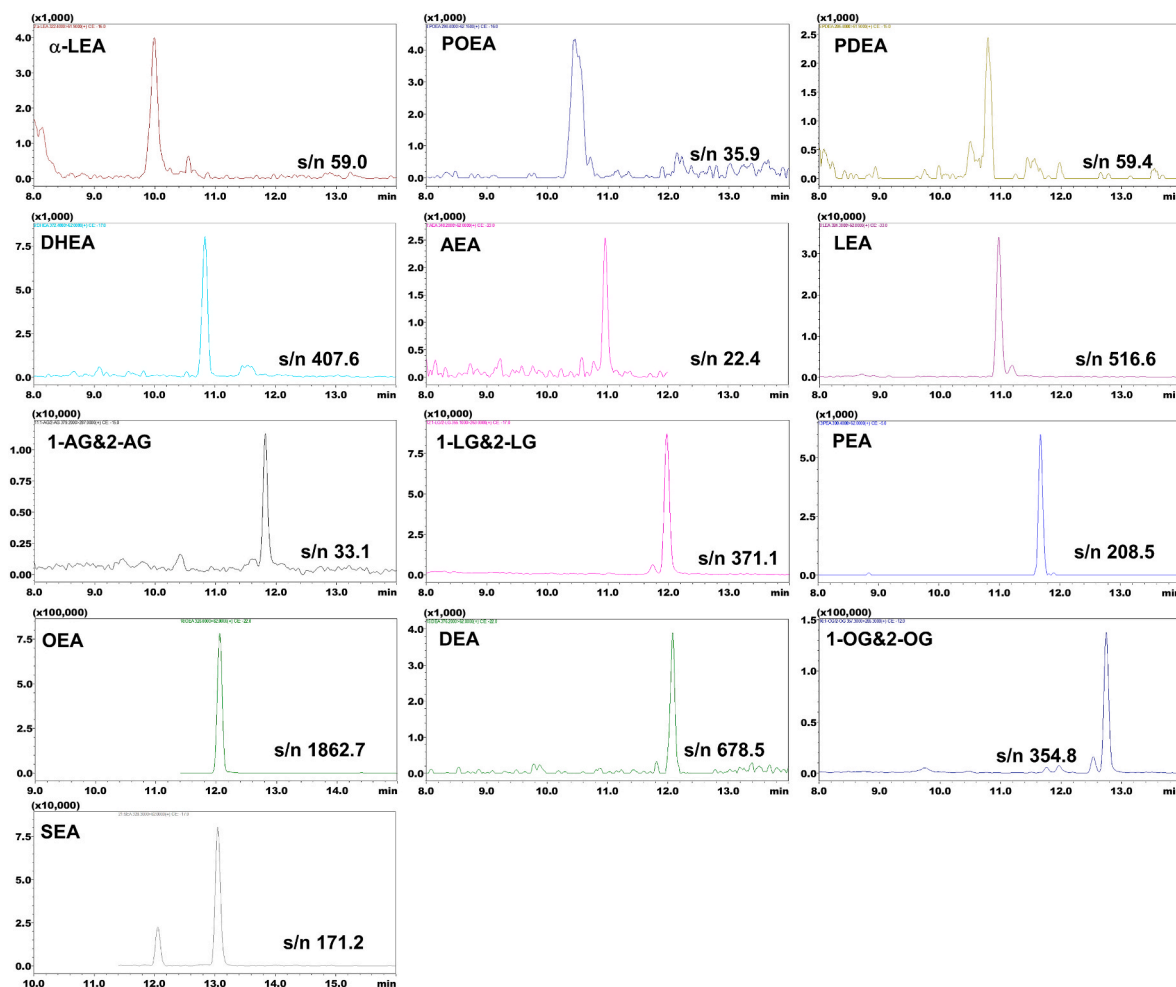


Fig. 5. SRM chromatograms of eCBs and eCB analogues in pooled human CSF as determined by micro-LC-MS/MS using a flow rate of $4 \mu\text{L min}^{-1}$ and an injection volume of $3 \mu\text{L}$. The x-axis is retention time and the y-axis is the detector response signal.

broadening, may be amplified. In this study, the spray emitter was connected to fused silica tubing ($50 \mu\text{L}$ I.D., 60-cm length) with well-fitting sleeves and a zero dead volume union. Although the total add-on volume was around $1.2 \mu\text{L}$, no significant peak broadening or shifting was observed during the analysis.

The micro-LC gradient was optimized based on previous work [19]. The injection volume was evaluated based on column capacity, signal intensity and peak shape. Initial mobile phase was used as injection solvent since it resulted in the best peak shape. Next, MS parameters including nebulizing gas, heating gas, interface temperature, interface voltage, collision energy and dwell time were further optimized with standard solution. The optimized LC-MS parameters are described in Section 2.7. After the optimization of micro-LC-MS/MS conditions, all the targeted compounds were separated with nice peak shape by using a Phenomenex C18 ($2.6 \mu\text{m}$, $0.3 \times 150 \text{ mm}$) column with 16 min analysis time (Fig. 4). Typical SRM chromatograms of targeted eCBs and eCB analogues in human CSF are shown in Fig. 5. It is worth mentioning that due to the volume of mobile phase mixer, online filter, and tubings in micro-LC system, gradients could not reach the column immediately at a flow rate of $4 \mu\text{L min}^{-1}$, which results in a delay of the retention time. Such delay, however, will not affect the peak shape or method repeatability.

3.3. Analytical performance evaluation

The optimized method in Section 2.7 was validated according to the EMA guidelines for the validation of analytical methods [24], with

Table 4

Intraday and interday precision (RSD%).

compounds	Intraday precision (%)			Interday precision (%)		
	Low	Medium	High	Low	Medium	High
d_8 -AEA	10.9%	0.3%	0.1%	13.7%	2.7%	3.8%
d_8 -2-AG	3.2%	2.2%	4.6%	10.9%	9.6%	6.3%
d_4 -OEA	9.8%	8.8%	2.3%	13.7%	6.7%	2.2%
d_4 -LEA	0.3%	1.6%	2.3%	10.1%	5.4%	10.2%
d_4 -DHEA	9.2%	5.5%	9.3%	10.1%	5.4%	10.2%
d_4 -PEA	6.5%	6.2%	3.8%	11.0%	13.5%	6.4%
d_3 -SEA	4.2%	0.9%	0.2%	6.1%	8.6%	5.7%

evaluation of linearity, precision, recovery and matrix effects. The calibration ranges were determined according to the levels observed in test samples as well as the information retrieved from the Human Metabolome Database (HMDB) and literature [11–17,20,31–34]. The linearity, LOD and LOQ are summarized in Table 3. Precision (intraday and interday) values, recovery and matrix effects are summarized in Table 4.

The coefficient of determination (R^2) values are all between 0.995 and 0.999 (significance $F < 0.05$), and at least 75% of the back calculated concentrations of the calibration standards were within $\pm 15\%$ (20% for LOQ) of the nominal value, indicating that the linearity was satisfactory for all the analytes. The LOQs were between 2.0 and 152.4 pM for most of the compounds, with the exception of PEA. A study reported that PEA contained in polyurethane foam, which is used for the

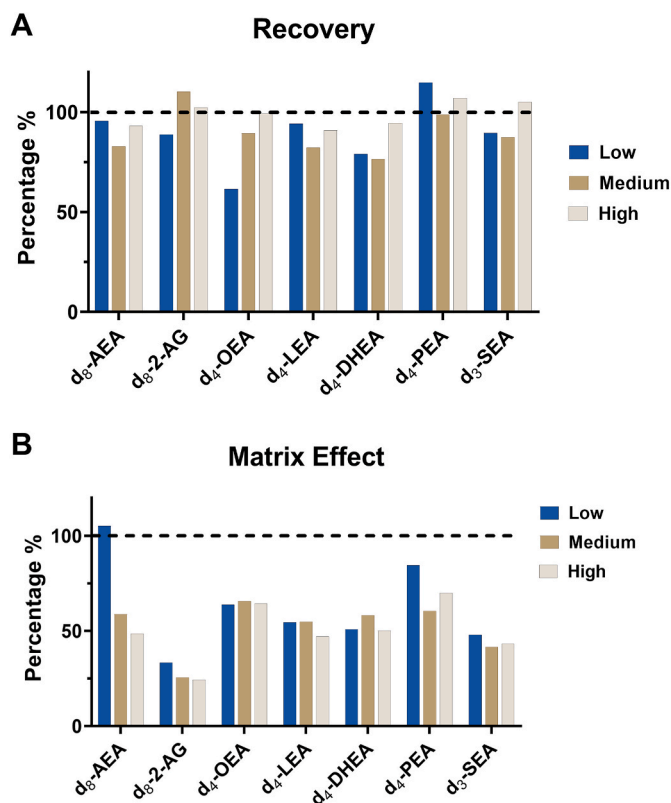


Fig. 6. Recovery and matrix effect of deuterated internal standards in human CSF. Recovery and matrix effect values are expressed in percentages. (A) Recovery: higher values indicate better recoveries. (B) Matrix effect: values above 100% imply ion enhancement and below 100% imply ion suppression.

wrapping material for some experimental glassware, can be absorbed by the glass and later on released to organic solvent during sample preparation [35]. Another report showed that plastic material could also be contaminated by NAEs including PEA [36]. It is important to monitor background contamination of this class to avoid jeopardizing the quantification accuracy of these compounds in biological samples. We observed noticeable PEA peaks in blank sample (50% ACN) and in the lowest calibrant of the calibration curve. Hence, the contamination of PEA from laboratory materials can explain its abnormally high LOD and LOQ values.

The intraday and interday precision were assessed using three different concentrations [low-level (C2), medium-level (C4), and high-level (C6)] of internal standards spiked in pooled CSF. Triplicate samples were prepared in each batch, and three batches were measured in three consecutive days. Intra- and interday precisions varied from 0.1% to 10.9% and from 2.2% to 13.7%, respectively, which are all within

15%, indicating that the repeatability was within the tolerance limits (Table 4). These results are comparable to previously reported quantification methods for eCBs with nano-flow LC-MS [19], as well as some methods with conventional LC-MS. In addition, during the analysis of the 288 CSF samples, no significant signal decrease was observed, which also demonstrated the robustness of this method.

Recovery and matrix effect were determined using deuterated internal standards. The recoveries ranged from 61.5% to 114.8%. Matrix effects ranged from 24.4% to 105.2% (Fig. 6). All compounds showed acceptable recovery. Major matrix effects were observed for several analytes, which may be caused by co-eluting phospholipids. As deuterated ISTDs were used, the quantification accuracy was ensured.

3.4. Application to the analysis of human CSF samples

As part of another study, CSF samples were collected in a population of males and females with an age ranging from 18 to 69 and measured using the developed micro-LC-MS/MS method. The study was conducted according to the criteria of the Declaration of Helsinki and was approved by the Leiden University Medical Center institutional ethics committee. All participants provided written informed consent prior to participation in the study. Data obtained from the healthy controls ($n = 94$) is reported in current study. The concentration distributions of AEA and 2-AG in the 94 healthy control samples and their correlation with gender and age are shown in Fig. 7. Concentration of AEA in this CSF study for healthy controls ranged from 1.0 to 7.1 pM, and for 2-AG from 87.9 to 658.5 pM. These levels can be used as future reference in follow-up studies. Significant correlation was observed between age and 2-AG concentration in healthy females (p -value = 0.026). However, no clear correlation was observed between age and the concentration of AEA in human CSF. Although it should be noted that confounding factors might have affected the relation as we did not take these into account. Moreover, the quantification results showed that this method is robust and sensitive enough to be applied to future clinical studies.

4. Conclusion

In this study, we developed and optimized a novel micro-LC-MS/MS method for the determination of eCBs and their analogues in human CSF. By using AEA and 1-AG/2-AG as reference compounds, the comparison of conventional and micro-level flow rates highlighted the advantage of micro-flow in increasing the sensitivity for targeted compounds. The flow rate was down scaled to $4 \mu\text{L min}^{-1}$ with a 0.3-mm inner diameter column, other setting and parameters were also optimized correspondingly to adapt the micro-flow. A minor modification on Shimadzu Mikros Micro-ESI spray needle was carried out to improve the robustness of this method. Requiring 250 μL CSF, the method reached LODs ranging from 0.6 to 1293.4 pM and LOQs ranging from 2.0 to 4311.3 pM. The repeatability was within the tolerance limits, with intraday and interday precisions under 13.7%. The developed micro-LC-

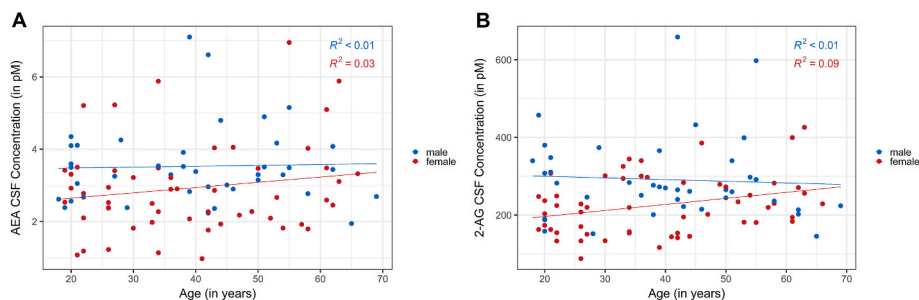


Fig. 7. Correlation between compounds and age based on the quantification data using the validated micro-LC-MS/MS method. The colors represent male (blue) and female (red). R^2 = coefficient of determination. (For interpretation of the references to color in this figure legend, the reader is referred to the Web version of this article.)

MS/MS method was found to be fit-for-purpose for the analysis of clinical CSF samples, in which 288 human CSF samples were successfully measured. With the wider coverage of eCBs and high robustness for CSF analysis, our method showed its applicability for future clinical research of brain disorders in which a disturbance in the ECS can be expected.

CRedit authorship contribution statement

Bingshu He: Methodology, Validation, Data curation, Formal analysis, Writing – original draft. **Xinyu Di:** Methodology, Validation, Data curation, Formal analysis, Writing – review & editing. **Faisa Guled:** Methodology, Conceptualization. **Aster V.E. Harder:** Resources, Formal analysis, Writing – review & editing. **Arn M.J.M. van den Maagdenberg:** Resources, Writing – review & editing. **Gisela M. Terwindt:** Resources, Writing – review & editing. **Elke H.J. Krekels:** Writing – review & editing. **Isabelle Kohler:** Writing – review & editing. **Amy Harms:** Conceptualization, Writing – review & editing, Supervision. **Rawi Ramautar:** Conceptualization, Writing – review & editing. **Thomas Hankemeier:** Conceptualization, Writing – review & editing, Supervision, Funding acquisition.

Declaration of competing interest

The authors declare that they have no known competing financial interests or personal relationships that could have appeared to influence the work reported in this paper.

Acknowledgements

This study was supported by the China Scholarship Council (CSC, No. 201906390032 to Bingshu He and CSC, No. 201707060012 to Xinyu Di). Dr. Rawi Ramautar would like to acknowledge the financial support of the Vidi grant scheme of the Netherlands Organization of Scientific Research (NWO Vidi 723.016.003). This work was also supported by the Netherlands Organization for Health Research and Development (Vidi grant no. 917-11-31 to GMT), and European Community (EC) funded FP7-EUROHEADPAIN (grant no. 602633 to AMJMvdM). This research was part of the Netherlands X-omics Initiative and partially funded by NWO, project 184.034.019.

Appendix A. Supplementary data

Supplementary data to this article can be found online at <https://doi.org/10.1016/j.aca.2022.339888>.

References

- [1] F.A. Iannotti, V. Di Marzo, S. Petrosino, Endocannabinoids and endocannabinoid-related mediators: targets, metabolism and role in neurological disorders, *Prog. Lipid Res.* 62 (2016) 107–128.
- [2] S. Ben-Shabat, E. Fride, T. Sheskin, T. Tamiri, M.-H. Rhee, Z. Vogel, T. Bisogno, L. De Petrocellis, V. Di Marzo, R. Mechoulam, An entourage effect: inactive endogenous fatty acid glycerol esters enhance 2-arachidonoyl-glycerol cannabinoid activity, *Eur. J. Pharmacol.* 353 (1998) 23–31.
- [3] W.-S. Ho, D.A. Barrett, M.D. Randall, 'Entourage' effects of N-palmitoylethanolamide and N-oleoylethanolamide on vasorelaxation to anandamide occur through TRPV1 receptors, *Br. J. Pharmacol.* 155 (2008) 837–846.
- [4] R. Greco, C. Demartini, M. Francavilla, A.M. Zanaboni, C. Tassorelli, Dual inhibition of FAAH and MAGL counteracts migraine-like pain and behavior in an animal model of migraine, *Cells* 10 (2021) 2543.
- [5] A. Della Pietra, R. Giniatullin, J.R. Savinainen, Distinct activity of endocannabinoid-hydrolyzing enzymes MAGL and FAAH in key regions of peripheral and central nervous system implicated in migraine, *Int. J. Mol. Sci.* 22 (2021) 1204.
- [6] E. Kilinc, S. Ankarali, I.E. Torun, Y. Dagistan, Receptor mechanisms mediating the anti-neuroinflammatory effects of endocannabinoid system modulation in a rat model of migraine, *Eur. J. Neurosci.* 55 (4) (2022 Feb) 1015–1031, <https://doi.org/10.1111/ejn.14897>.
- [7] C. Tassorelli, R. Greco, S.D. Silberstein, The endocannabinoid system in migraine: from bench to pharmacy and back, *Curr. Opin. Neurol.* 32 (2019) 405–412.
- [8] J. Mulder, M. Zilberter, S.J. Pasquaré, A. Alpár, G. Schulte, S.G. Ferreira, A. Köfalvi, A.M. Martín-Moreno, E. Keimpema, H. Tanila, M. Watanabe, K. Mackie, T. Hortobágyi, M.L. de Ceballos, T. Harkany, Molecular reorganization of endocannabinoid signalling in Alzheimer's disease, *Brain* 134 (2011) 1041–1060.
- [9] C. Altamura, M. Ventriglia, M.G. Martini, D. Montesano, Y. Errante, F. Piscitelli, F. Scarscia, C. Quattrocchi, P. Palazzo, S. Seccia, F. Vernieri, V. Di Marzo, Elevation of plasma 2-arachidonoylglycerol levels in Alzheimer's disease patients as a potential protective mechanism against neurodegenerative decline, *J. Alzheim. Dis.* 46 (2015) 497–506.
- [10] P. Leimuranta, L. Khirouf, R. Giniatullin, Emerging role of (Endo)Cannabinoids in migraine, *Front. Pharmacol.* 9 (2018).
- [11] M. Di Filippo, L.A. Pini, G.P. Pelliccioli, P. Calabresi, P. Sarchielli, Abnormalities in the cerebrospinal fluid levels of endocannabinoids in multiple sclerosis, *J. Neurol. Neurosurg. Psychiatr.* 79 (2008) 1224–1229.
- [12] K.R. Müller-Vahl, L. Bindila, B. Lutz, F. Musshoff, T. Skripuletz, C. Baumgaertel, K.-W. Sühs, Cerebrospinal fluid endocannabinoid levels in Gilles de la Tourette syndrome, *Neuropsychopharmacology* 45 (2020) 1323–1329.
- [13] J. Nicholson, S. Azim, M.J. Rebecchi, W. Galbavy, T. Feng, R. Reinsel, S. Rizwan, C. J. Fowler, H. Benveniste, M. Kaczocha, Leptin levels are negatively correlated with 2-arachidonoylglycerol in the cerebrospinal fluid of patients with osteoarthritis, *PLoS One* 10 (2015) e0123132-e0123132.
- [14] P. Sarchielli, L.A. Pini, F. Coppola, C. Rossi, A. Baldi, M.L. Mancini, P. Calabresi, Endocannabinoids in chronic migraine: CSF findings suggest a system failure, *Neuropsychopharmacology* 32 (2007) 1384–1390.
- [15] R. Jumpertz, A. Guijarro, R.E. Pratley, D. Piomelli, J. Krakoff, Central and peripheral endocannabinoids and cognate acylethanolamides in humans: association with race, adiposity, and energy expenditure, *J. Clin. Endocrinol. Metab.* 96 (2011) 787–791.
- [16] A. Romigi, M. Bari, F. Placidi, M.G. Marciani, M. Malaponti, F. Torelli, F. Izzi, C. Prosperetti, S. Zannino, F. Corte, C. Chiamonte, M. Maccarrone, Cerebrospinal fluid levels of the endocannabinoid anandamide are reduced in patients with untreated newly diagnosed temporal lobe epilepsy, *Epilepsia* 51 (2010) 768–772.
- [17] C. Marchioni, B.L. Santos-Lobato, M.E.C. Queiroz, J.A.S. Crippa, V. Tumas, Endocannabinoid levels in patients with Parkinson's disease with and without levodopa-induced dyskinesias, *J. Neural. Transm.* 127 (2020) 1359–1367.
- [18] J. Nicholson, S. Azim, M.J. Rebecchi, W. Galbavy, T. Feng, R. Reinsel, S. Rizwan, C. J. Fowler, H. Benveniste, M. Kaczocha, Leptin levels are negatively correlated with 2-arachidonoylglycerol in the cerebrospinal fluid of patients with osteoarthritis, *PLoS One* 10 (2015), e0123132.
- [19] V. Kanta, S. Ogino, M. Noga, A.C. Harms, R.M. van Dongen, G.L.J. Onderwater, A. M.J.M. van den Maagdenberg, G.M. Terwindt, M. van der Stelt, M.D. Ferrari, T. Hankemeier, Quantitative profiling of endocannabinoids and related N-acylethanolamines in human CSF using nano LC-MS/MS, *JLR (J. Lipid Res.)* 58 (2017) 615–624.
- [20] J. Czepiel, J. Gdula-Argasińska, G. Biesiada, B. Bystrowska, A. Jurczyszyn, W. Perucki, K. Sroczyńska, A. Zajac, T. Librowski, A. Garlicki, Fatty acids and selected endocannabinoids content in cerebrospinal fluids from patients with neuroinfections, *Metab. Brain Dis.* 34 (2019) 331–339.
- [21] F.M. Leweke, A. Giuffrida, D. Koethe, D. Schreiber, B.M. Nolden, L. Kranaster, M. A. Neatby, M. Schneider, C.W. Gerth, M. Hellmich, J. Klosterkötter, D. Piomelli, Anandamide levels in cerebrospinal fluid of first-episode schizophrenic patients: impact of cannabis use, *Schizophr. Res.* 94 (2007) 29–36.
- [22] A.E. Kirby, M.J. Jebrail, H. Yang, A.R. Wheeler, Folded emitters for nano-electrospray ionization mass spectrometry, *Rapid Commun. Mass Spectrom.* 24 (2010) 3425–3431.
- [23] Y. Huang, Q. Zhang, Y. Liu, B. Jiang, X. Jie, T. Gong, B. Jia, X. Liu, J. Yao, W. Cao, H. Shen, P. Yang, Aperture-controllable nano-electrospray emitter and its application in cardiac proteome analysis, *Talanta* 207 (2020), 120340.
- [24] E.E.M. Agency, in: E.M. Agency (Ed.), Guidelines for the Validation of Analytical Methods Used in Residue Depletion Studies, 2009.
- [25] A. Shrivastava, V.B. Gupta, Methods for the determination of limit of detection and limit of quantitation of the analytical methods, *Chronicles Young Sci.* 2 (2011) 15–21.
- [26] J. Zhang, W. Shou, T. Ogura, S. Li, H. Weller, Optimization of microflow LC-MS/MS and its utility in quantitative discovery bioanalysis, *Bioanalysis* 11 (2019) 1117–1127.
- [27] M. Hilhorst, C. Briscoe, N.v.d. Merbel, Sense and nonsense of miniaturized LC-MS/MS for bioanalysis, *Bioanalysis* 6 (2014) 3263–3265.
- [28] A. Schmidt, M. Karas, T. Dülcks, Effect of different solution flow rates on analyte ion signals in nano-ESI MS, or: when does ESI turn into nano-ESI? *J. Am. Soc. Mass Spectrom.* 14 (2003) 492–500.
- [29] H. Liu, G. Raffin, G. Trutt, J. Randon, Is vacuum ultraviolet detector a concentration or a mass dependent detector? *J. Chromatogr. A* 1530 (2017) 171–175.
- [30] K.L. Sanders, J.L. Edwards, Nano-liquid chromatography-mass spectrometry and recent applications in omics investigations, *Anal. Methods* 12 (2020) 4404–4417.
- [31] M. Bobrich, R. Schwarz, R. Ramer, P. Borchert, B. Hinz, A simple LC-MS/MS method for the simultaneous quantification of endocannabinoids in biological samples, *J. Chromatogr. B* 1161 (2020), 122371.
- [32] I. Mennella, M. Savarese, R. Ferracane, R. Sacchi, P. Vitaglione, Oleic acid content of a meal promotes oleoylethanolamide response and reduces subsequent energy intake in humans, *Food Funct.* 6 (2015) 203–209.
- [33] R. Ottria, A. Ravelli, F. Gigli, P. Ciuffreda, Simultaneous ultra-high performance liquid chromatography-electrospray ionization-quadrupole-time of flight mass

- spectrometry quantification of endogenous anandamide and related N-acylethanolamides in bio-matrices, *J. Chromatogr. B* 958 (2014) 83–89.
- [34] P.J.H. Jones, L. Lin, L.G. Gillingham, H. Yang, J.M. Omar, Modulation of plasma N-acylethanolamine levels and physiological parameters by dietary fatty acid composition in humans, *J. Lipid Res.* 55 (2014) 2655–2664.
- [35] Identification of a widespread palmitoylethanolamide contamination in standard laboratory glassware, *Cannabis Cannabinoid Res.* 2 (2017) 123–132.
- [36] S. Oddi, F. Fezza, G. Catanzaro, C. De Simone, M. Pucci, D. Piomelli, A. Finazzi-Agro, M. Maccarrone, Pitfalls and solutions in assaying anandamide transport in cells[S], *JLR (J. Lipid Res.)* 51 (2010) 2435–2444.